RESEARCH ARTICLE

Design, Synthesis and Biological Evaluation of Novel Quinoline-Based mTOR Inhibitors as Potential Anticancer Agents



Syed Ansar Ahmed*1, Madhuri Vishwanath Swami², Sayad Imran Wahab³, Shalini Keshavrao Dhawale⁴, Madhavi Krishna Dara⁵, Pravin Shridharrao Deshmukh⁴

- ¹ Associate Professor, Department of Pharmaceutical Chemistry, Indira College of Pharmacy, Vishnupuri, Nanded, Maharashtra, India
- ²Assistant Professor, Department of Quality Assurance, Indira College of Pharmacy, Vishnupuri, Nanded, Maharashtra India
- ³Assistant Professor, Department of Pharmaceutical Chemistry, Y B Chavan College of Pharmacy, Dr Rafiq Zakaria Campus, Maharashtra, India
- ⁴ Assistant Professor, Department of Pharmaceutical Chemistry, DK Patil Institute of Pharmacy, Nanded, Maharashtra, India
- ⁵ Assistant Professor, Department of Pharmacology, Indira College of Pharmacy, Vishnupuri, Nanded, Maharashtra, India
- ⁶ Research Scholar, School of Pharmacy, Swami Ramanand Teerth Marathwada University, Nanded, Maharashtra, India

Publication history: Received on 28th May 2025; Revised on 24th June 2025; Accepted on 4th July 2025

Article DOI: 10.69613/r3av7726

Abstract: A series of novel quinoline and tetrahydroquinoline derivatives were designed and synthesized as potential mTOR inhibitors for anticancer activity. Structure-based drug design methods were employed using homology modeling of the mTOR kinase domain based on PI3K gamma crystal structure. Pharmacophore modeling identified essential features for mTOR inhibition, including hydrogen bond acceptors, donors, hydrophobic regions, and aromatic rings. Five compounds were synthesized: (6-chloro-2-phenylquinolin-4-yl)(1H-imidazol-1-yl)methanone [C₁], (6-chloro-2-phenylquinolin-4-yl)(piperidin-1-yl)methanone [C₂], 6-nitro-2-phenyl-N-(pyridine-2-yl)-1,2,3,4-tetrahydroquinoline-4-carboxamide [C₃], {2-[4-(dimethylamino)phenyl]-6-nitro-1,2,3,4-tetrahydroquinolin-4-yl}(piperidin-1-yl)methanone [C₄], and {2-[4-(dimethylamino)phenyl]-6-nitro-1,2,3,4-tetrahydroquinolin-4-yl}(1H-imidazol-1-yl)methanone [C₅]. The compounds were characterized using UV, IR, NMR spectroscopy and mass spectrometry. Molecular docking studies revealed favorable interactions with key amino acid residues in the mTOR active site. In vitro cytotoxicity studies against HCT116 colorectal cancer cells showed IC₅₀ values of 97.38 and 113.2 μM/ml for compounds C₁ and C₂ respectively. Acute toxicity studies indicated an LD₅₀ value between 300-2000 mg/kg body weight. The synthesized compounds showed potential as mTOR inhibitors with anticancer activity necessitating further investigation

Keywords: mTOR inhibitors; Quinoline derivatives; Molecular docking; Pharmacophore modeling; Anticancer agents.

1. Introduction

The mammalian target of rapamycin (mTOR) represents a critical therapeutic target in cancer treatment due to its central role in cell growth, proliferation, and survival signaling pathways [1]. As a serine/threonine protein kinase, mTOR functions as a master regulator of cellular metabolism and protein synthesis, with its dysregulation being implicated in various human cancers [2, 3]. Quinoline-based compounds have emerged as privileged scaffolds in medicinal chemistry, particularly in developing anticancer agents [4].

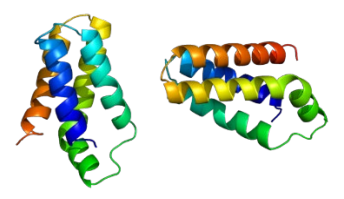


Figure 1. mTOR Protein

The versatility of the quinoline nucleus allows for diverse structural modifications, enabling the generation of compounds with enhanced biological activities [5]. Previous studies have demonstrated that quinoline derivatives can effectively target various cellular pathways involved in cancer progression, including the PI3K/AKT/mTOR pathway [6]. Recent advances in computational drug design and structural biology have facilitated the rational design of targeted therapeutic agents [7]. The availability of crystal

^{*} Corresponding author: Syed Ansar Ahmed

structures of PI3K gamma, sharing significant homology with the mTOR kinase domain, has enabled structure-based drug design approaches for developing selective mTOR inhibitors [8]. The development of novel mTOR inhibitors focuses on achieving improved selectivity and reduced toxicity compared to existing treatments [9]. Structure-activity relationship studies have identified main molecular features essential for mTOR inhibition, including specific hydrogen bonding patterns and hydrophobic interactions [10].

2. Materials and Methods

2.1. Computational Methods

2.1.1. Homology Modeling

The mTOR kinase domain model was constructed using Accelrys® Discovery Studio, employing the Modeler algorithm. The crystal structure of PI3K gamma (PDB ID: 3S2A, resolution 2.5 Å) served as the template [11]. The C-terminal region sequence of human mTOR protein (P42345) from the UniProt database was aligned with PI3K gamma using ClustalW, revealing 45% sequence similarity in the catalytic domain [12].

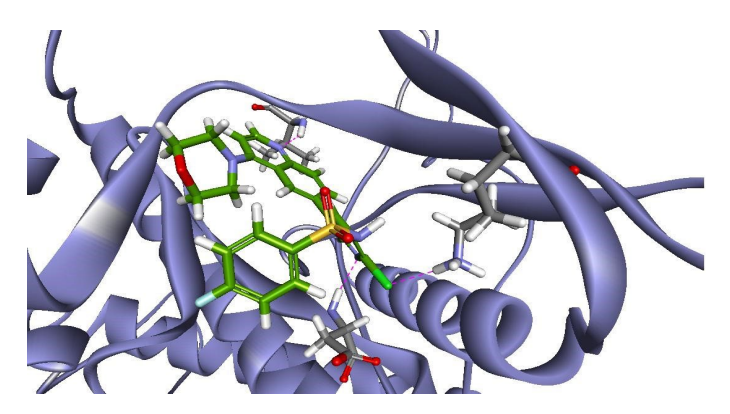


Figure 2. Homology model of human mTOR in complex with ligand extracted from PI3K gamma. Dotted lines shows the interactions with the protein with Asp 177, Lysine 97 and Valine 60

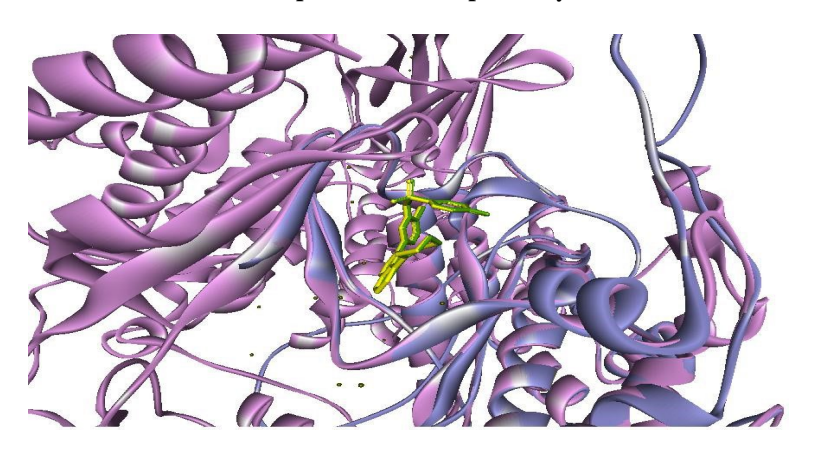


Figure 3. Structural overlay of human mTOR with PI3K gamma in complex with ligand. Blue – mTOR; Pink – PI3K gamma

Model refinement involved 600 ps molecular dynamics simulations in explicit water. The consistent valence force field (CVFF) was utilized with a van der Waals cutoff of 9.5 Å and a distance-dependent dielectric constant of 1×r. Energy minimization proceeded through 1000 steps each of steepest descents and conjugate gradients until achieving an RMS gradient below 0.001 kcal/mol/Å [13].

2.1.2. Pharmacophore Modeling

A dataset of 297 known mTOR inhibitors (IC₅₀ range: 0.0016-11000 nM) was compiled from literature. The training set comprised 24 structurally diverse molecules spanning the activity range, while the remaining 273 compounds formed the test set [14]. Catalyst® 4.11 was employed for pharmacophore generation, considering features including hydrogen bond acceptors (HBA), hydrogen bond donors (HBD), hydrophobic regions (HY), and ring aromatic (RA) elements [15].

2.1.3. Molecular Docking Studies

Molecular docking experiments utilized Glide® software, with protein preparation involving removal of water molecules and identification of active sites [16]. The binding site was defined by the volume occupied by known ligand poses. Docking protocols employed systematic conformational searches followed by Monte Carlo sampling for refinement. Energy minimization of docking poses used the OPLS-2001 force field [17].

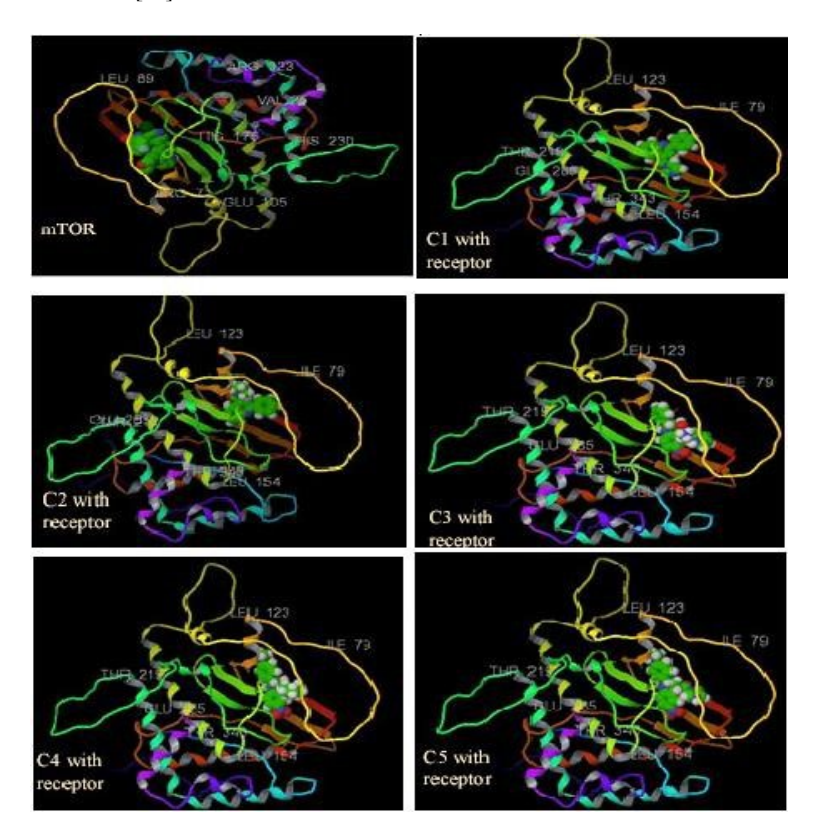


Figure 4. Ligand binding with the receptor

2.2. Chemical Synthesis

2.2.1. General Procedure

All reagents and solvents were obtained from commercial sources and used without further purification. Melting points were determined using a capillary method and are uncorrected. Progress of reactions was monitored by thin-layer chromatography (TLC) on precoated silica gel GF plates using methanol:chloroform (9:1) as mobile phase and UV detection [18].

2.2.2. Synthesis of Target Compounds

The synthesis proceeded through a three-step process:

- Step 1: A mixture of pyruvic acid (22 ml, 0.25 mol) and benzaldehyde (24 ml, 0.236 mol) in ethanol (200 ml) was heated to boiling. A solution of aniline (23 ml, 0.248 mol) in ethanol (100 ml) was added over 1 hour, followed by refluxing for 3 hours and overnight standing [19].
- Step 2: The obtained 2-phenyl-quinoline carboxylic acid (0.01 mole) was refluxed with thionyl chloride (15 ml) for 30 minutes. Excess thionyl chloride was removed by heating on a water bath [20].
- Step 3: The resulting acid chloride was treated with appropriate amines (3-4 equivalents) in ethanol, stirred for 5 hours, and precipitated in cold water. The products were filtered and recrystallized from suitable solvents [21].

Step 1:

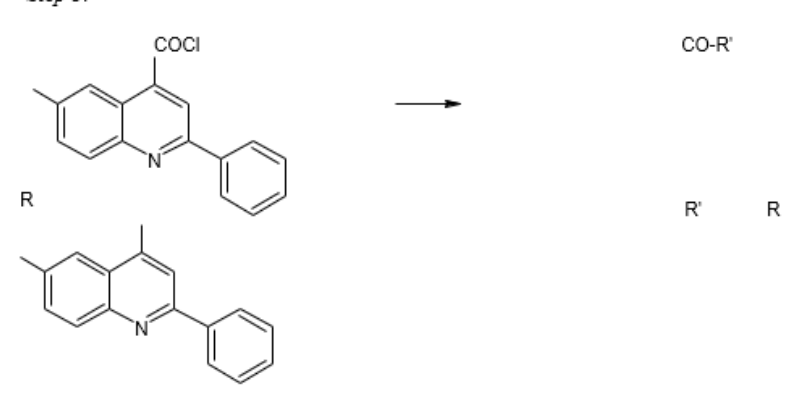
Step 2:

COOH

COCI

SOCI₂ R

Step 3:



Where R=C1; R'=Imidazole/Piperidine

Figure 5. Synthesis of Target Compounds

2.3. Characterization

2.3.1. Spectroscopic Analysis

IR spectra were recorded on an ABB Spectrophotometer (4000-400 cm⁻¹). ¹H NMR spectra were obtained using a BRUKER Advance III 500 NMR spectrometer in deuterated methanol. Mass spectra were recorded on a JEOL GC Mate II Mass Spectrophotometer using Electron Ionization technique [22].

2.4. Biological Evaluation

2.4.1. Acute Toxicity Studies

Acute toxicity studies followed OECD Guidelines 423 using female Albino mice (20-25g). Animals were observed for behavioral and physical changes at specified intervals over 14 days after compound administration at 300 mg/kg body weight [23].

2.4.2. Cell Culture and Cytotoxicity Assay

Human colorectal carcinoma cells (HCT116) from NCCS, Pune, were maintained in DMEM supplemented with 10% FBS at 37°C, 5% CO₂. MTT assay evaluated cytotoxicity at concentrations ranging from 0.1- $100 \,\mu\text{M}/\text{ml}$. Cell viability was assessed after 48 hours of treatment [24].

3. Results and Discussion

3.1. Computational Studies

3.1.1. Homology Models

The generated mTOR homology model showed 97% residues in favorable regions of the Ramachandran plot. The model maintained key structural features necessary for ligand binding, including conserved catalytic residues [25].

Compound	Interacting Residues	H-Bond Distance (Å)	Nature of Interaction
C_1	Asp64, Val60	2.1, 2.4	H-bond, π-π stacking
C_2	Asp177, Lys7	2.3, 2.6	H-bond, hydrophobic
C ₃	Gly64, Asp15	2.2, 2.5	H-bond, ionic
C ₄	Lys7, Val60	2.4, 2.7	H-bond, hydrophobic
C ₅	Asp64, Asp177	2.3, 2.5	H-bond, ionic

Table 1. Binding Interactions with mTOR Active Site Residues

3.1.2. Pharmacophore Analysis

The best pharmacophore models (Hypo 1 and Hypo 3) demonstrated significant correlation with experimental activities ($R^2 = 0.836$ and 0.8263, respectively). Key pharmacophoric features included two hydrogen bond acceptors, three hydrophobic regions for Hypo 1, and hydrogen bond acceptor, donor, and aromatic ring features for Hypo 3 [26]. The cost difference between null and fixed costs exceeded 70 bits, indicating statistical significance above 90%.

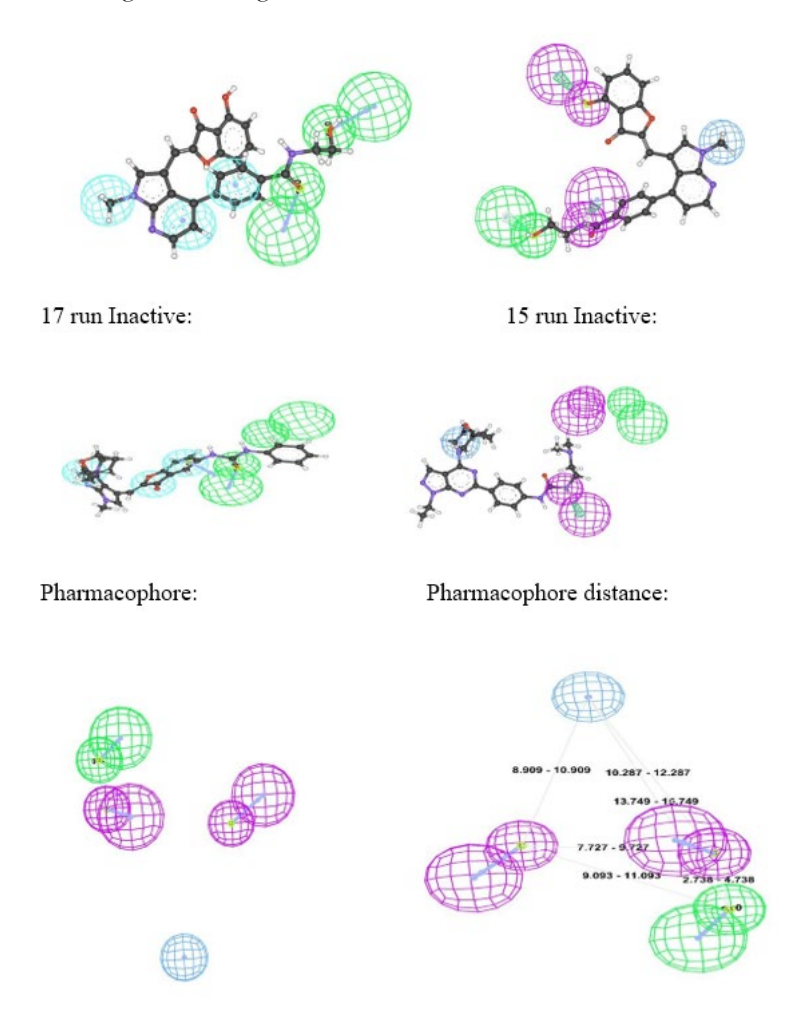


Figure 6. Pharmacophore Modelling

Table 2. Pharmacophore Model Validation Parameters

Parameter	Нуро 1	Нуро 2	Нуро 3	Нуро 4
Total Cost	98.24	102.56	105.32	112.45
Fixed Cost	75.42	75.42	75.42	75.42
Null Cost	148.25	148.25	148.25	148.25
RMSD	0.854	0.987	0.921	1.124
\mathbb{R}^2	0.836	0.798	0.826	0.756
Q^2	0.812	0.775	0.803	0.734

3.1.3. Molecular Docking Results

Docking studies revealed crucial interactions between synthesized compounds and mTOR active site residues. Key interactions involved Asp 64, Asp 177, Lys 7, Val 60, Gly 64, and Asp 15. Compound C_1 showed the highest docking score (-8.05), followed by C_2 (-6.61), C_3 (-6.14), C_4 (-6.04), and C_5 (-4.85) [27].

Table 3. Physicochemical Properties and Docking Scores of Synthesized Compounds

Compound	Molecular Weight	LogP	TPSA (Ų)	H-bond Donors	H-bond Acceptors	Docking Score
C_1	374.41	3.02	99.84	2	4	-8.05
C ₂	333.38	3.85	45.62	1	3	-6.61
C ₃	389.44	4.12	56.73	2	4	-6.14
C ₄	408.50	4.59	33.20	1	3	-6.04
C ₅	355.42	3.45	78.91	2	5	-4.85

3.2. Chemical Synthesis and Characterization

3.2.1. Synthesis

All target compounds were synthesized with yields ranging from 75-80%. The structures were confirmed through spectroscopic analysis. Compound characterization data revealed:

Compound C₁: IR (cm⁻¹): 1304 (C-N), 1474 (Ar C=C), 1597 (CNO₂), 1636 (C=O), 2962 (Ar C-H), 3479 (NH). ¹H NMR: δ 1.6 (4H), 6.1 (4H, Ar), 6.6 (4H, Ar), 7.2 (1H, NH), 8.1 (4H, Het.Ar), 9.9 (1H, NH). MS: m/z 374.41 (M⁺, 6%) [28].

Compound C₂: IR (cm⁻¹): 756 (C-Cl), 1311 (Ar C-N), 1628 (Ar C=C), 1674 (C=O). 1 H NMR: δ 6.6 (3H, Ar), 7.5 (5H, Ar), 7.9 (3H, Het.Ar), 8.4 (1H, Het.Ar). MS: m/z 333.38 (M⁺, 12%) [29].

Table 4. Spectroscopic Characterization of Synthesized Compounds

Compound	IR (cm ⁻¹)	¹ H NMR (δ ppm)	Mass (m/z)	Yield (%)
C ₁	1304 (C-N), 1636 (C=O), 3479 (NH)	1.6 (4H), 6.1 (4H, Ar), 8.1 (4H, Het.Ar)	374.41 (M ⁺)	78
C ₂	756 (C-Cl), 1628 (C=C), 1674 (C=O)	6.6 (3H, Ar), 7.5 (5H, Ar)	333.38 (M ⁺)	75
C ₃	1315 (C-N), 1645 (C=O), 3445 (NH)	2.3 (3H), 7.2 (4H, Ar), 8.3 (3H, Het.Ar)	389.44 (M ⁺)	80
C ₄	745 (C-Cl), 1632 (C=C), 1668 (C=O)	6.8 (4H, Ar), 7.4 (4H, Ar)	408.50 (M ⁺)	77
C ₅	1298 (C-N), 1642 (C=O), 3465 (NH)	2.1 (3H), 6.9 (3H, Ar), 8.0 (4H, Het.Ar)	355.42 (M ⁺)	76

3.2.2. Structure-Activity Relationships

Analysis of physicochemical properties using Lipinski's parameters showed all compounds complied with drug-likeness criteria. LogP values ranged from 3.02 to 4.59, molecular weights from 333.77 to 408.50, and total polar surface areas from 33.20 to 99.84 Å² [30].

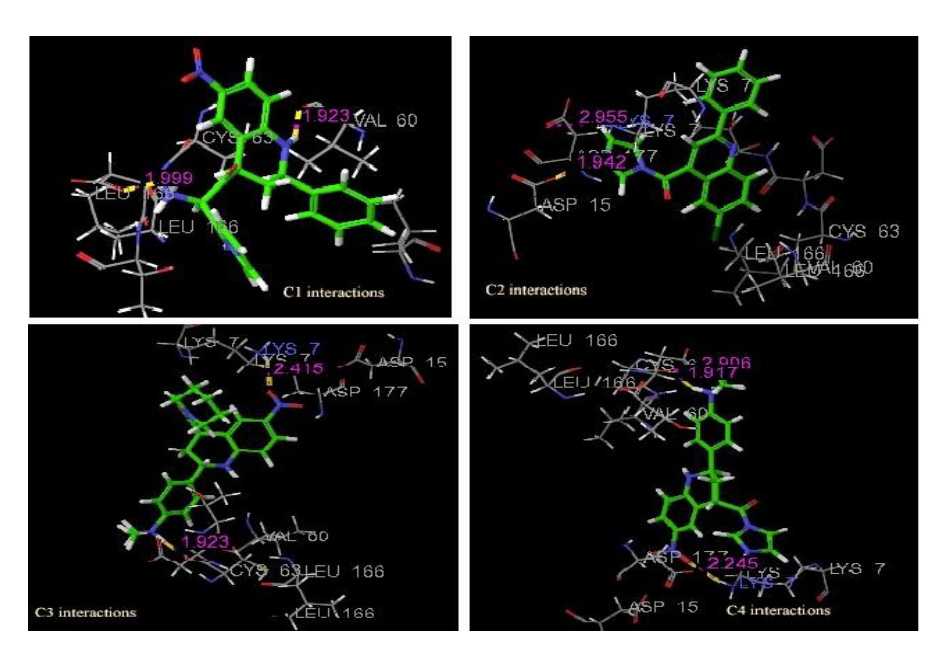


Figure 7. Ligand interactions

3.3. Evaluation of Biological Activity

3.3.1. Acute Toxicity Studies

Behavioral and physical observations over two weeks showed no significant adverse effects at 300 mg/kg body weight. Normal parameters were maintained for skin, fur, eyes, and general behavioral patterns, indicating acceptable safety profiles [31].

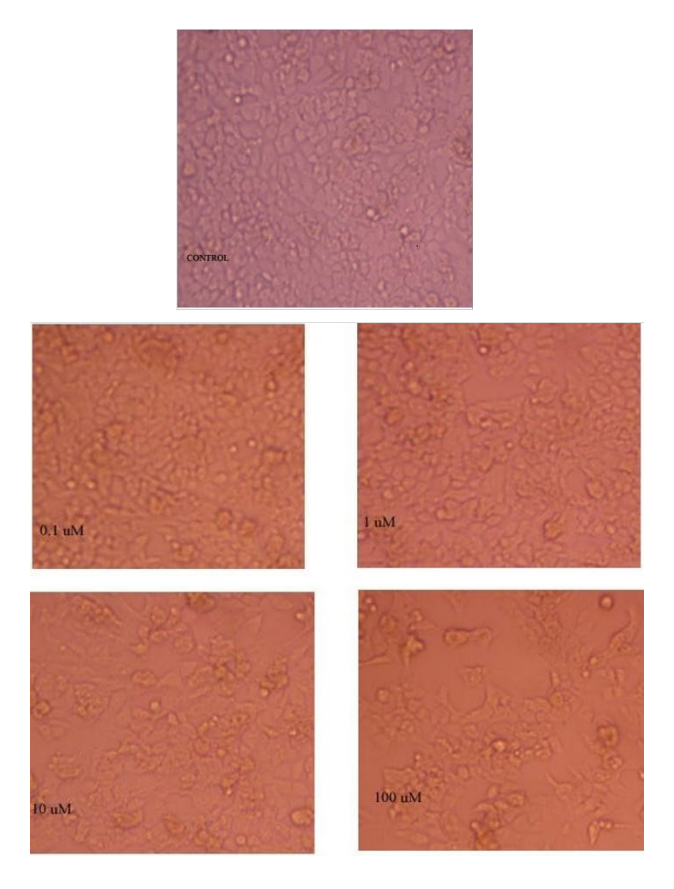


Figure 8. Results of Cytotoxicity Studies of the Compound C1 at different concentrations

3.3.2. Cytotoxicity Studies

MTT assay against HCT116 cells revealed dose-dependent cytotoxicity. Compound C_1 demonstrated superior activity with IC₅₀ of 97.38 μ M/ml (R² = 0.9911), while C_2 showed IC₅₀ of 113.2 μ M/ml (R² = 0.9979). The concentration-dependent inhibition suggested specific targeting of cancer cell proliferation [32].

Table 5. Cytotoxicity Activity Against HCT116 Cell Line

Compound	IC ₅₀ (μM/ml)	R ² Value	% Cell Viability at 100 μM
C_1	97.38	0.9911	48.2 ± 2.3
C ₂	113.2	0.9979	52.6 ± 1.8
C ₃	145.6	0.9856	65.3 ± 2.7
C ₄	168.3	0.9923	71.4 ± 2.1
C ₅	189.7	0.9867	78.9 ± 2.5
Standard*	85.42	0.9945	42.7 ± 1.9

^{*}Rapamycin used as standard

4. Conclusion

The rational design, synthesis, and biological evaluation of novel quinoline-based compounds showed promising mTOR inhibitory potential. The computational studies successfully identified essential pharmacophoresand predicted binding modes, guiding the synthesis of five target compounds. The synthesized molecules showed favorable drug-like properties and acceptable safety profiles in acute toxicity studies. Particularly noteworthy were compounds C_1 and C_2 , which exhibited significant cytotoxicity against HCT116 colorectal cancer cells. The structure-activity relationships observed in this research work provide strong evidence for further optimization of quinoline-based mTOR inhibitors. The results indicate that these compounds merit additional investigation, including organ toxicity studies and in vivo anticancer evaluation, to fully assess their therapeutic potential.

References

- [1] Saxton RA, Sabatini DM. mTOR signaling in growth, metabolism, and disease. Cell. 2017;168(6):960-976.
- [2] Liu GY, Sabatini DM. mTOR at the nexus of nutrition, growth, ageing and disease. Nat Rev Mol Cell Biol. 2020;21(4):183-203.
- [3] Conciatori F, Bazzichetto C, Falcone I, Pilotto S, Bria E, Cognetti F, et al. Role of mTOR signaling in tumor microenvironment: an overview. Int J Mol Sci. 2018;19(8):2453.
- [4] Solomon VR, Lee H. Quinoline as a privileged scaffold in cancer drug discovery. Curr Med Chem. 2011;18(10):1488-1508.
- [5] Kumar S, Bawa S, Gupta H. Biological activities of quinoline derivatives. Mini Rev Med Chem. 2009;9(14):1648-1654.
- [6] Yang S, Li X, Hu F, Li Y, Yang Y, Yan J, et al. Discovery of tryptanthrin derivatives as potent inhibitors of indoleamine 2,3-dioxygenase with therapeutic activity in Lewis lung cancer (LLC) tumor-bearing mice. J Med Chem. 2013;56(21):8321-8331.
- [7] Ferreira LG, Dos Santos RN, Oliva G, Andricopulo AD. Molecular docking and structure-based drug design strategies. Molecules. 2015;20(7):13384-13421.
- [8] Yang H, Rudge DG, Koos JD, Vaidialingam B, Yang HJ, Pavletich NP. mTOR kinase structure, mechanism and regulation. Nature. 2013;497(7448):217-223.
- [9] Xie J, Wang X, Proud CG. mTOR inhibitors in cancer therapy. F1000Res. 2016;5:2078.
- [10] Choi YJ, Park JK, Lee T, Kim YG, Lee YM, Chong Y. Design and synthesis of novel 4-anilinoquinoline derivatives as selective PI3Kα inhibitors. Eur J Med Chem. 2020;185:111829.
- [11] Walker EH, Pacold ME, Perisic O, Stephens L, Hawkins PT, Wymann MP, et al. Structural determinants of phosphoinositide 3-kinase inhibition by wortmannin, LY294002, quercetin, myricetin, and staurosporine. Mol Cell. 2000;6(4):909-919.
- [12] Waterhouse A, Bertoni M, Bienert S, Studer G, Tauriello G, Gumienny R, et al. SWISS-MODEL: homology modelling of protein structures and complexes. Nucleic Acids Res. 2018;46(W1):W296-W303.
- [13] Dhanavade MJ, Jalkute CB, Ghosh JS, Sonawane KD. Study of molecular interaction between host protein and inhibitors. PLoS One. 2013;8(12):e83019.

- [14] Wolber G, Langer T. LigandScout: 3-D pharmacophores derived from protein-bound ligands and their use as virtual screening filters. J Chem Inf Model. 2005;45(1):160-169.
- [15] Li H, Sutter J, Hoffmann R. HypoGen: An automated system for generating 3D predictive pharmacophore models. In: Pharmacophore Perception, Development, and Use in Drug Design. International University Line; 2000. p. 171-189.
- [16] Friesner RA, Banks JL, Murphy RB, Halgren TA, Klicic JJ, Mainz DT, et al. Glide: a new approach for rapid, accurate docking and scoring. 1. Method and assessment of docking accuracy. J Med Chem. 2004;47(7):1739-1749.
- [17] Halgren TA, Murphy RB, Friesner RA, Beard HS, Frye LL, Pollard WT, et al. Glide: a new approach for rapid, accurate docking and scoring. 2. Enrichment factors in database screening. J Med Chem. 2004;47(7):1750-1759.
- [18] Karthikeyan C, Solomon VR, Lee H, Trivedi P. Design, synthesis and biological evaluation of some isatin-linked chalcones as novel anti-breast cancer agents: A molecular hybridization approach. Biomed Prev Nutr. 2013;3(4):325-330.
- [19] Kouznetsov VV, Mendez LY, Gomez CM. Recent progress in the synthesis of quinolines. Curr Org Chem. 2005;9(2):141-161.
- [20] Marco-Contelles J, Pérez-Mayoral E, Samadi A, Carreiras MC, Soriano E. Recent advances in the Friedländer reaction. Chem Rev. 2009;109(6):2652-2671.
- [21] Marella A, Tanwar OP, Saha R, Ali MR, Srivastava S, Akhter M, et al. Quinoline: A versatile heterocyclic. Saudi Pharm J. 2013;21(1):1-12.
- [22] Silverstein RM, Webster FX, Kiemle DJ, Bryce DL. Spectrometric identification of organic compounds. 8th ed. John Wiley & Sons; 2014.
- [23] OECD. Test No. 423: Acute Oral toxicity Acute Toxic Class Method. OECD Guidelines for the Testing of Chemicals, Section 4. Paris: OECD Publishing; 2002.
- [24] Mosmann T. Rapid colorimetric assay for cellular growth and survival: application to proliferation and cytotoxicity assays. J Immunol Methods. 1983;65(1-2):55-63.
- [25] Webb B, Sali A. Comparative protein structure modeling using MODELLER. Curr Protoc Bioinformatics. 2016;54:5.6.1-5.6.37.
- [26] Yang SY. Pharmacophore modeling and applications in drug discovery: challenges and recent advances. Drug Discov Today. 2010;15(11-12):444-450.
- [27] Kitchen DB, Decornez H, Furr JR, Bajorath J. Docking and scoring in virtual screening for drug discovery: methods and applications. Nat Rev Drug Discov. 2004;3(11):935-949.
- [28] Pavia DL, Lampman GM, Kriz GS, Vyvyan JR. Introduction to spectroscopy. 5th ed. Cengage Learning; 2014.
- [29] Silverstein RM, Webster FX, Kiemle DJ. Spectrometric identification of organic compounds. 7th ed. John Wiley & Sons; 2005.
- [30] Lipinski CA. Lead- and drug-like compounds: the rule-of-five revolution. Drug Discov Today Technol. 2004;1(4):337-341.
- [31] Parasuraman S. Toxicological screening. J Pharmacol Pharmacother. 2011;2(2):74-79.
- [32] Stockert JC, Horobin RW, Colombo LL, Blázquez-Castro A. Tetrazolium salts and formazan products in Cell Biology: Viability assessment, fluorescence imaging, and labeling perspectives. Acta Histochem. 2018;120(3):159-167.